Astron. Astrophys. 356, 529–540 (2000)

ASTRONOMY AND ASTROPHYSICS

Wide binaries among high-velocity and metal-poor stars⋆

C. Allen, A. Poveda, and M.A. Herrera

Instituto de Astronomía, UNAM, Apartado Postal 70-264, México, D.F. 04510

Received 23 June 1999 / Accepted 9 December 1999

Abstract. A catalogue of 122 wide binaries is presented. The list was compiled by searching for common proper-motion companions to the more than 1200 high-velocity and metal-poor stars of Schuster and collaborators. We study the separations for the wide binaries ($\langle a \rangle > 25$ AU), and find that they follow Oepik's distribution all the way up to 10 000 AU. A subgroup of them, the ones with the most halo-like orbits, follow Oepik's distribution up to 20 000 AU. The galactic orbits of all systems are calculated, and galactic orbital parameters are used, along with the metallicites, to assign each one to the old thin disk, the thick disk, or the halo population.

Key words: catalogs – stars: binaries: general – stars: Population II – Galaxy: halo

1. Introduction

The properties of old disk and halo binaries are of interest for the understanding of the processes of formation and early dynamical evolution of the Galaxy. The luminosity function of the components of wide binaries and multiples, their mass function, the fraction of halo or old disk stars that are members of wide binaries, and the distribution of their separations are some of the basic properties that are poorly understood, mainly because of the paucity of known wide binaries among halo and old disk stars.

The question relative to the fraction of stars that are members of binaries or multiple systems as a function of their kinematics (or age) has been present since Oort (1926) pointed out the paucity of visual binaries among high-velocity stars. Various authors have addressed this problem in the past, mainly with the purpose of establishing the fraction of binaries (of all separations) among halo stars, without specific regard to the fraction of visual binaries. For instance, Carney (1983), by means of a photometric study of high-velocity stars, found that 20-25% of such stars are close binaries, considerably less than the corresponding fraction for ordinary disk stars. Stryker et al. (1985) found, from spectroscopic data for a sample of high-velocity stars, a lower limit of 20-30% for the binary frequency among these stars. This value, of course, refers only to spectroscopic binarity, and is again considerably lower than for disk stars. Recent investigations about the incidence of wide binaries (visual and common-proper-motion companions) are few. Abt & Willmarth (1987) noted 6 wide binaries among 45 high-velocity dwarfs, while Martin & Rebolo (1992) found 7 companions (with angular separations ranging from $1''$ to $60''$) in CCD images of 51 low-metallicity or high-velocity stars ([Fe/H]< -1) taken from Laird et al. (1988) and Schuster & Nissen (1989b). So far, the largest sample of binaries among Population II stars is that obtained by Ryan (1992), who did UBVRI photometry of common-proper-motion stars from the NLTT catalogue (Luyten 1979, 1980). Ryan's search produced some 25 wide binaries with good photometry, but for them neither trigonometric parallaxes nor radial velocities are available, so no reliable kinematic studies can be made.

In this paper we are particularly interested in wide binaries ($a > 25$ AU), as opposed to close binaries ($a < 25$ AU), for several reasons. First, wide binaries seem to be the result of a process of formation different from that of closer binaries (Abt & Levy 1976; Poveda et al. 1997; Allen et al. 1997). Second, wide binaries, because of their small binding energies, are good sensors of unknown mass concentrations that may encounter them throughout their galactic trajectories. In this respect, the dynamic history of halo binary stars may well be distinct from that of disk stars.

In the present work we have elaborated a list of 115 systems containing a total of 122 wide binaries, mostly belonging to the halo or thick disk, by searching for common-proper-motion companions to the high-velocity and metal-poor stars studied by Schuster and collaborators (SN: Schuster & Nissen 1988; SPC: Schuster et al. 1993). Based on Stromgren photometry, Schuster et al. have derived distances, metallicities and ages for their stars. Since each star has a large and well determined proper motion it was possible to compare this value with that of NLTT stars of its vicinity. Each system was carefully checked to avoid misidentifications, and when appropriate, distances were updated using the Hipparcos trigonometric parallaxes.

We have determined the distribution of angular separations for our wide binaries. Reliable distances are available for all of

Send offprint requests to: Christine Allen (chris@astroscu.unam.mx)

⋆ Table 2 is only available in electronic form at the CDS via anonymous ftp to cdsarc.u.strasbg.fr (130.79.128.5) or via http://cdsweb.u-strasbg.fr/Abstract.html

our systems, so this distribution can be converted into a distribution of separations in AU. We find 11 systems that have projected separations in excess of 10 000 AU, or 15 systems with expected semiaxes larger than 10 000 AU; the existence of these very wide binaries poses interesting dynamical problems. Since many systems have known radial velocities, space velocities for them can be determined, and their galactic orbits computed and characterized. The secondaries of these wide binaries are interesting in themselves, since they represent a sampling of the faint end of the main sequence of old disk and halo stars.

2. Construction of the catalogue

For each star of the SN and SPC catalogues a machine search for common-proper-motion companions was made among the NLTT stars within 12 minutes of arc. Although a tolerance was initially given for the proper motions differences, it was found that the common-proper-motion companions had, in fact, proper motions identical to those of the primaries to the last significant digit in the NLTT. This initial list was checked to avoid errors due to misidentifications, duplicate entries, etc., and was supplemented with some companions listed in the LDS (Luyten 1987) and not present in the NLTT (mostly from the southern hemisphere), as well as with additional common-proper-motion companions found in the CCDM (Dommanget & Nys 1994). Additional close companions found in the CCDM were retained only if an orbit was given, or if their separations were of less than $1''$. In the latter case the likelihood of their being physically associated with their primaries is high. Wider companions were usually eliminated, unless convincing evidence of their sharing the proper motion of the primary was found. A case in point is the well-known multiple system Rho Geminorum (Hipparcos 36366); Hipparcos observed the two brightest stars, and found for them common proper motions and parallaxes; however, we found no convincing evidence that the other two wide companions have the same proper motions. Hence, we list it as a triple. Another interesting case is the pair composed of G89-13 and G89-14 (Hipparcos 35750-35756); both these stars have the same proper motion; however, their parallaxes, as determined by Hipparcos are very different; also, the radial velocities of both components differ significantly (Sandage & Fouts 1987); hence, the pair G89-13/G89-14 was eliminated from our catalogue. However, G89-14 has another common proper-motion companion, which was retained.

The total number of entries in our list is 131. Of these, 122 correspond to wide binaries, that is, binaries with expected major semiaxes larger than 25 AU. Many of these companions had already been identified as common-proper-motion companions by Luyten.

Angular separations between the components were mostly taken from the Notes of the NLTT, supplemented by the LDS, the Gliese-Jahreiss (1991) catalogue, and the CCDM. As mentioned above, close companions were usually retained in the catalogue. Many of these companions turn out to have physical separations of less than 25 AU, and they were excluded from the following discussions.

Distances to the primaries were taken, when appropriate, from the Hipparcos catalogue. Hipparcos distances were adopted for those stars with relative errors in their trigonometric parallaxes of less than 15%. For stars with larger errors, the photometric distances were preferred; these were kindly provided by W. J. Schuster. They were determined in the way described by Schuster & Allen (1997). The method involves the derivation of E(b-y) and [Fe/H] using the intrinsic-color and metallicity calibrations of Schuster & Nissen (1989a). Procedures for de-reddening the photometry are given in Schuster & Nissen (1989a, 1989b). Photometric distances were then calculated using the calibration of Nissen & Schuster (1991), which takes into account evolutionary corrections (Nissen et al. 1987). In Column 16 (Notes) of Table 2 in the Appendix the provenance of the parallax is indicated. Note that Hipparcos parallaxes were adopted for the great majority of the systems listed.

Absolute visual magnitudes for the primaries were calculated from the adopted distances and the apparent visual magnitudes given by Schuster and collaborators (in SN and SPC). Absolute visual magnitudes for the secondaries were calculated from the apparent red and photographic (blue) magnitude differences between the components, $\delta(m_R)$, $\delta(m_B)$, as estimated by Luyten. These $\delta(m)$ were transformed to visual magnitude differences by means of relations derived for those NLTT stars that also have reliable photometry in the visual band, as listed in the Gliese-Jahreiss catalogue (1991). The relations used are (Lavalley 1994):

$$\delta V_B = 0.972\delta(m_B), \qquad \delta V_R = 1.055\delta(m_R).$$

The absolute visual magnitudes of the secondaries were then calculated from those of the primaries by adding the calculated $\delta V = (1/2)(\delta V_B + \delta V_R)$.

The procedure we used to determine the absolute visual magnitudes for the secondaries is thus based on an accurate photometric magnitude for the primary, and magnitude differences (in two colors) for the secondary. Although the magnitudes estimated by Luyten in his catalogues are somewhat uncertain, the magnitude *differences* between the components of a binary are usually more accurate, and hence the derived absolute magnitudes for the secondaries should also be better. In order to check the accuracy of these magnitudes we searched for binaries in our list that have independent photometry of both components in the Hipparchos and Tycho catalogues. We found 19 such pairs. A comparison between the so observed magnitude differences and the δV calculated by us is shown in Fig. 1. The figure shows no systematic trend; the mean of the differences is 0.07 mag, with a dispersion of 0.30 mag. Note that this value is significantly smaller than the dispersion determined by Ryan (1989) for the magnitudes of individual stars as estimated by Luyten, which is about 0.6 mag.

Linear separations between the components were calculated from the angular separations and the adopted distances. The linear separations were transformed into expected values for the major semiaxes by means of the statistical relation (Couteau 1960)

$$E(\log a) - E(\log s) = 0.146.$$

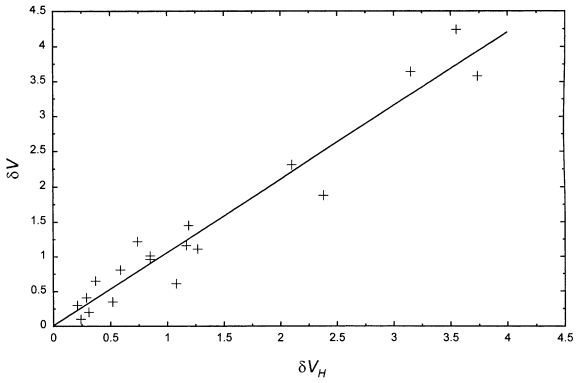

Fig. 1. Visual magnitude differences between primaries and secondaries as determined by our method (ordinate), and as observed by Hipparcos (abscissa). The straight line is the linear regression to the points.

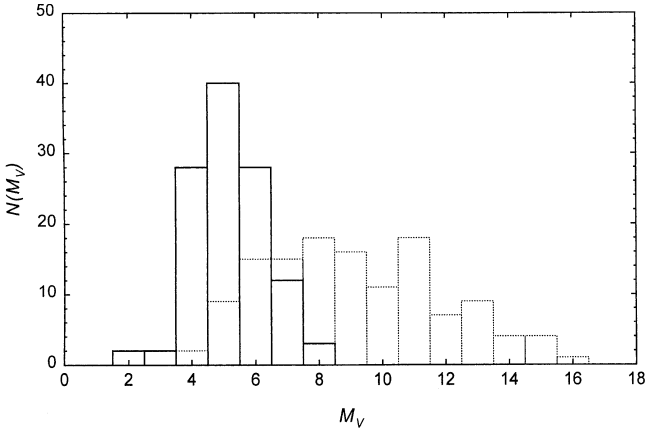

Fig. 2. Frequency distribution of the absolute visual magnitudes of the primaries (full line) and of the secondaries (dotted line).

In the following, a wide binary with a projected angular separation s''_{AB} between components A and B is assumed to have an "expected" major semiaxis $\langle a \rangle$ in AU, given by

$$\langle a \rangle = \text{antilog} \left[\log \frac{s''_{AB}}{\pi} + 0.146 \right],$$

were π is the parallax.

The catalogue is presented in Table 2, available in electronic form. Each line stands for a binary system; triples are listed as two lines, i.e., as two binaries. The first column contains the Hipparcos number of the primary, when available. Column 2 contains other identifications of the star; we list, in order of preference, numbers in the HD, the Giclas (G) or the Wilson catalogues (W). In the third column the multiplicity is indicated. Column 4 contains the distance to the primary, taken from the Hipparcos catalogue when the relative error in the trigonometric parallax was less than 15%; when the Hipparcos errors were larger (this occurs mostly for the more distant stars) the photometric distances given by Schuster and collaborators were preferred. The distances to all the components of a system were assumed to be equal to the distance to the primary. In one case, HD 112573, Hipparcos determined an accurate trigonometric parallax for the secondary, and hence this was taken also for the primary. Columns 5 and 6 contain the absolute visual magnitudes of the primary and secondary, respectively, determined as described above. The angular separation between the components is given in Column 7, and the expected value of the major semiaxes in Column 8. Columns 9 and 10 contain the metallicity of the primary and its age, as determined by Schuster and collaborators. The individual ages listed were kindly provided by W. J. Schuster; they are based on the isochrones of VandenBerg (1985). The peculiar velocity of the binary is given in Column 11. To compute the peculiar velocities a solar motion of (9, 12, 7) km s^{-1} was assumed. Radial velocities were taken from various sources in the literature; detailed references are given in Nissen & Schuster (1991) and in SPC (1993). Columns 12 to 14 contain the main galactic orbital parameters; we list the apocentric distance, R_{max}, as well as the maximum distance away from the galactic plane reached by the star $|z_{max}|$, and the three-dimensional eccentricity e of its galactic orbit.

Most of the stars in the Schuster et al. lists (and in similar catalogues) result from searches of stars from weak-line or large proper-motion catalogues; therefore, such stars are candidates to be either low-metallicity, or high-velocity, or both. Hence, they are likely to belong to either the halo or the thick disk. But it is by no means certain that an individual star will, after being more accurately observed, turn out to have a large space velocity, a low metallicity or a large age. To be comprehensive, we have retained all binaries in our catalogue; but care should be taken, when deriving properties pertaining to binaries of a certain kinematic or metallicity group, to exclude the stars not belonging to this group. A full discussion of the relationships of the galactic orbital parameters and the metallicity of different population groups is beyond the scope of the present paper, but a rough classification of the stars is given in Column 15. Only three population groups have been considered here, namely old thin disk (d), thick disk (td), and halo (h). We define and discuss these groups in Sect. 4 below.

3. Some statistical properties

Fig. 2 shows the frequency distribution of the absolute visual magnitudes of the primaries (full line) and of the secondaries (dotted line) of the binaries in the catalogue. Especially noteworthy in this figure is the very faint range of absolute magnitudes of the secondaries, which constitutes a sampling of the faint end of the main sequence for these old and/or metal poor stars.

Fig. 3 displays a plot of the U, V components of the peculiar velocities of the binaries in our sample. Note that the great majority of the stars have peculiar velocities in excess of 60 km s^{-1}, and can be considered therefore *bona fide* high-velocity stars. In fact, only 20 systems have peculiar velocities smaller than 60 km s^{-1}. Fig. 4 displays a histogram of the distribution of peculiar velocities.

The cumulative distribution of the observed angular separations of the wide binaries in our catalogue is shown in Fig. 5. On this plane, Oepik's distribution (Oepik 1924), $f(s) \propto 1/s$,

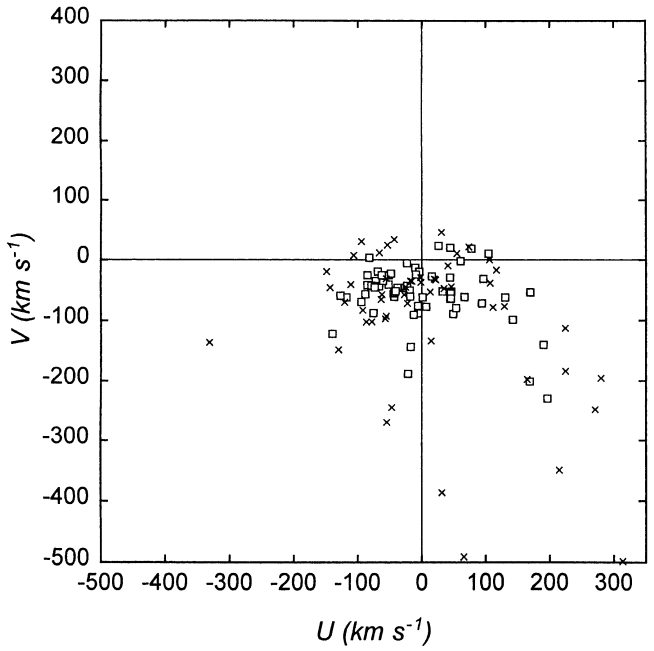

Fig. 3. Plot of the U, V components of the space velocities with respect to the Local Standard of Rest. Stars whose $|W|$ velocities are larger than 30 km s^{-1} are plotted as crosses, stars with smaller $|W|$ velocities as squares.

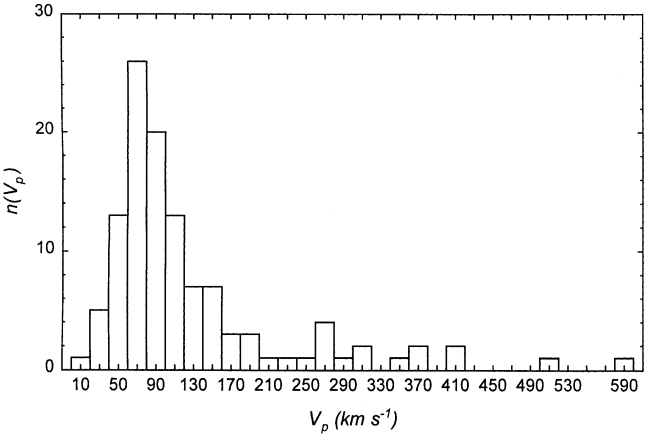

Fig. 4. Frequency distribution of the total peculiar velocities.

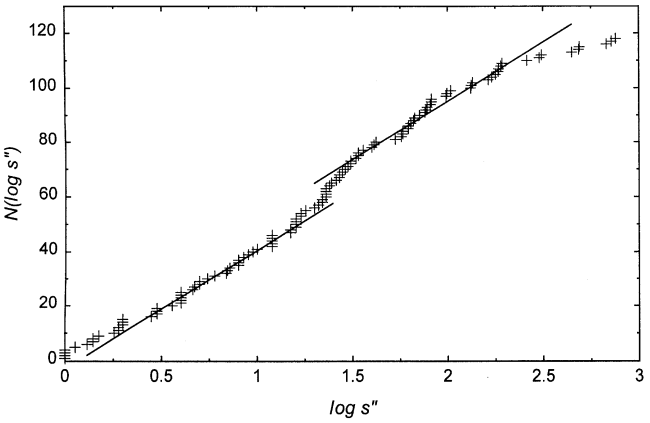

Fig. 5. Cumulative distribution of the observed angular separations of the binaries.

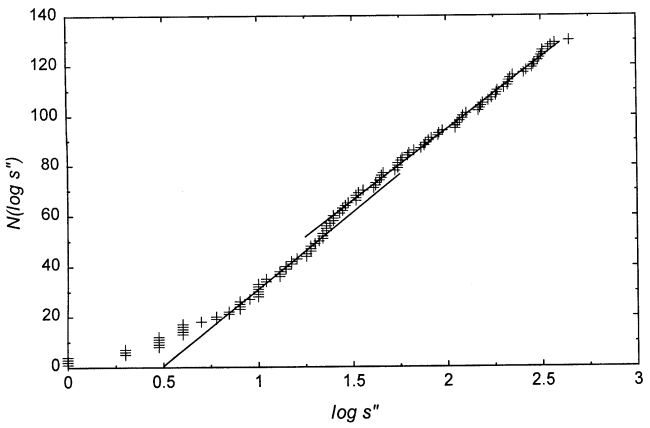

Fig. 6. Cumulative distribution of the observed angular separations of a subsample of wide binaries in the LDS catalogue.

is represented by a straight line whose parameters depend on normalization factors. Two fits are shown; the left-hand side fit corresponds to separations of less than 15 arc seconds, the right-hand side one to separations between 27 and 310 arc seconds. The region corresponding to the wider separations is probably more complete, since for closer separations many components become unobservable as common-proper-motion companions, especially when their magnitude differences are large.

It can be shown that if a group of wide binaries, exhibits a distribution of projected angular separations $f(s) \sim s^{-n}$, then the corresponding distribution of major semiaxes, $g(a)$, has also the form $g(a) \sim a^{-n}$; in the following, we will refer indistinctly to Oepik's distribution of angular separations, $f(s) \sim s^{-1}$, or of major semiaxes, $g(a) \sim a^{-1}$.

For comparison with Fig. 5, we show in Fig. 6 the cumulative distribution of the observed angular separations of a sample of wide binaries in the LDS catalogue. In order to have a sample of about the same size as that of our catalogue, only a representative declination zone was considered, namely between $+35$ and $+39$ degrees. It is clearly seen that this sample also follows Oepik's distribution. Again, two straight line fits are shown, corresponding to separations smaller than 22 and larger than 25 arc seconds. It is easily seen that very few stars with separations less than 15 arc seconds are present, because of the increasing difficulty of identifying faint proper-motion companions at such close separations.

The cumulative distribution of the expected values of the logarithms of the major semiaxes of the binaries in our catalogue is displayed in Fig. 7. On this plane too, Oepik's distribution is represented by a straight line. The change in slope that occurs at major semiaxes of about 1000 AU is probably due to incompleteness in the proper motion catalogues; this break corresponds to the discontinuity in the cumulative distribution of angular separations; as we have seen, this incompleteness sets in for separations smaller than about 15-20 arc seconds, especially for large $\delta(m)$. Indeed, the median angular separation of

the closer binaries ($\langle a \rangle$ smaller than about 1000 AU) is 4 arc sec, while for the wider binaries it is 72 arc sec.

To assess the significance of Oepik's distribution for the group of mostly very old binaries studied here, we stress that observational data show that the distribution of separations of very young systems seems to closely follow Oepik's relation from the time their component stars are established as separate entities within their condensing parent cloud (see Allen et al. 1997 for a recent discussion on this problem, and for references on the observational data). Combining observations from several studies on star-forming regions Larson (1995) found the surface density of companions to follow Oepik's relation at least up to 8000 AU. Furthermore, a study of a sample of wide binaries in the Orion Nebula cluster and in the Hyades (Nigoche 2000) showed that the distribution of separations seems to follow again Oepik's relation, up to $\langle a \rangle$ of 30 000 AU for the Orion Nebula cluster, and up to 18 000 AU for the Hyades cluster. The age of the Orion Nebula cluster is estimated to be a few million years (Hillenbrand 1997), that of the Hyades cluster 625 ± 50 My (Perryman et al. 1998). Also, our previous study on the distribution of separations of wide binaries in the solar neighborhood (Poveda et al. 1997) showed that even the oldest systems follow that distribution, albeit only to a critical $\langle a \rangle$ of 2400 AU. On the other hand, theoretical studies (Valtonen 1997) have indicated that Oepik's distribution results naturally for the binaries formed by dynamical interactions and desintegration of small star clusters.

Thus, there is ample observational evidence that perturbations due to encounters with massive objects will gradually deplete the distribution at the widest separations (most weakly bound pairs). The critical $\langle a \rangle$ at which the observed distribution departs from Oepik's is thus a function of the age of the group of binaries considered. In Sect. 5 below, we discuss the additional evidence in support of this evolutionary scenario contributed by the wide binaries studied in this paper, and we compare it with results on the binaries of the solar neighborhood found in our previous study.

The departure from Oepik's distribution observed for the present binaries at values of the expected semiaxes larger than about 10 000 AU is interpreted as due to the effects of dynamical interactions, which tend to decrease the binding energy, and hence the separation of the binary, until its ultimate dissolution. This departure sets in at a value considerably larger than that obtained for the old binaries of the solar vicinity (Poveda et al. 1997), which is about 2400 AU. This difference can be due to several effects. One is the relatively small time spent by the binaries of the present study (Table 1) within the galactic thin disk, which is where most of the dynamical effects are expected to take place. Another is the large relative velocity with which encounters with perturbers occur, resulting in smaller energy exchanges per encounter.

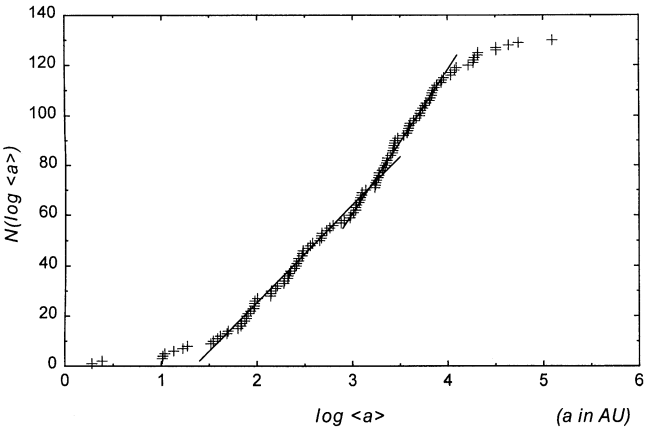

Fig. 7. Cumulative distribution of the expected values of the logarithms of the major semiaxes of the binaries in our catalogue.

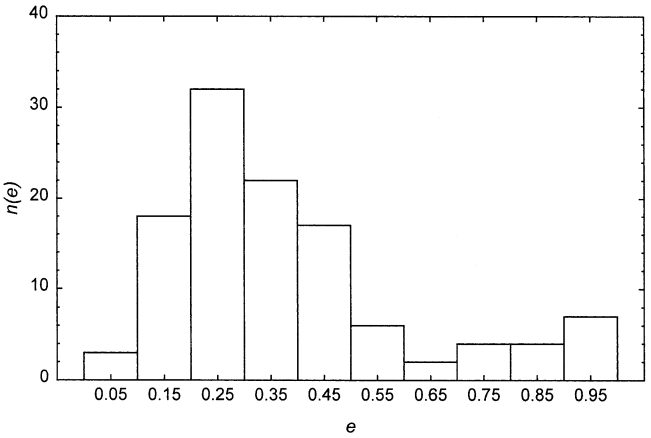

Fig. 8. Frequency distribution of the three-dimensional eccentricities of the galactic orbits of the binaries.

4. Galactic orbits

For all the wide binaries in our catalogue space velocities are available, and galactic orbits have been obtained using the potential of Allen & Santillán (1993). The orbits were numerically integrated backwards in time, for an interval corresponding to 1.6×10^{10} years, comparable to the age of the galactic halo or the old thin disk. Since the stars studied by Schuster and collaborators span a fairly wide range of kinematical properties and chemical composition, their membership to a given population group is not always clearly defined. Galactic orbital parameters are useful to better characterize the membership of a given star to different population groups. The main orbital parameters are given in Table 2, Columns 12 to 14. Fig. 8 shows the frequency distribution of the eccentricities, e, and Fig. 9 that of $|z_{max}|$, the maximum distances from the plane of the Galaxy reached by our wide binaries in their galactic orbits. It is seen that (out of 115 orbits) 48 stars have eccentricities larger than 0.35, and 51 stars reach values of $|z_{max}|$ of more than 500 pc.

For a rough classification of the stars into the three population groups indicated in Column 15 of Table 2, we used information on the metallicities, the kinematics and the orbital parameters. Full details are given in a forthcoming paper (Allen & Schuster 2000). In general, a star was assigned to the halo population either if it fell above the diagonal cut in the v_{rot} vs.

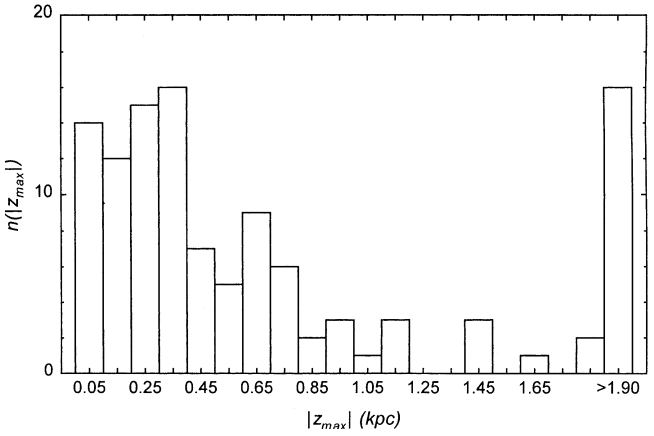

Fig. 9. Frequency distribution of $|z_{max}|$, the maximum distances from the galactic plane reached by the binaries in their galactic orbits.

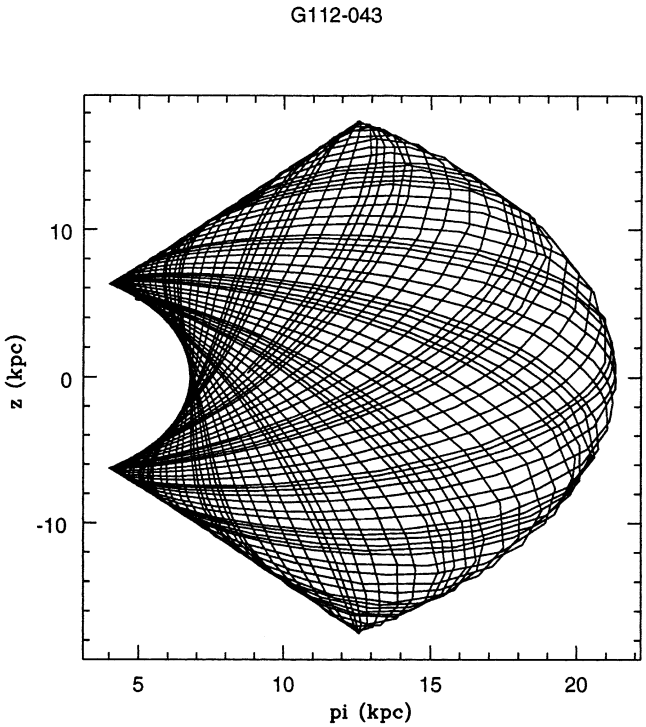

Fig. 10. Meridional galactic orbit of G112-43, an extreme halo system.

[Fe/H] diagram (SPC 1993) or if it had $|z_{max}| > 1000$ pc. After separating in this way the halo population, a star was assigned to the thick disk population if it had 1000 pc $> |z_{max}| > 500$ pc, or if its orbital eccentricity exceeded 0.35. In other cases the star was assigned to the old thin disk. It is seen that 30 binaries clearly belong to the halo population, 46 to the thick disk, and the remaining to the old (kinematically hot) thin disk.

Fig. 10 displays the meridional galactic orbit of the binary G112-43, an extreme halo system. Note that this system spends most of its time relatively far from the galactic plane, in regions where few dynamical interactions would be expected to occur.

Most of the orbits obtained are of regular type, but there are several examples of plunging orbits that reach pericentric distances so small as to make them of chaotic type. In such cases, energy exchanges between the motion on the galactic plane and the z–motion occur continuously, and the star can spend considerable lengths of time close to the plane, and then suddenly wander to distances of several kpc away from the plane. Examples of such behaviour are G2-38 and G106-25. Their meridional orbits and corresponding surfaces of section are shown in Figs. 11 and 12.

5. Discussion and conclusions

We have searched for common-proper-motion companions to the more than 1200 stars for which Schuster et al. obtained Stromgren photometry. For these stars, metallicities, photometric distances and (in some cases) ages are available. We have been able to identify 122 wide companions, for which good distances are available, many of them obtained from Hipparcos trigonometric parallaxes. The catalogue is presented in Table 2.

An analysis of the frequency distribution of the expected major semiaxes shows that they closely follow Oepik's distribution, namely, $f(a) \propto 1/a$. Two different sets of constants are observed for the range of major semiaxes considered, which seem to reflect the two main observational techniques employed in the discovery of wide binaries: searches for visual companions, and searches for common-proper-motion companions. We emphasize, however, that all of our listed wide companions are, in fact, common-proper-motion companions, and hence very likely to be physically associated.

As was found earlier for the binaries of the solar neighborhood, Oepik's distribution is followed only up to a critical major semiaxis. The departure from Oepik's distribution observed for the present binaries at values of the expected semiaxes larger than about 10 000 AU is interpreted as due to the effects of dynamical interactions, which tend to decrease the binding energy, and hence, to increase the separation of the binary, until its ultimate dissolution. This departure sets in at a value considerably larger than that obtained for the older binaries of the solar vicinity. In fact, we found the wide *younger* pairs (with mean ages of about 2.5 Gy) to follow Oepik's relation for major semiaxes of up to 8000 AU, whereas the wide *older* pairs (with mean ages of about 7 Gy) follow this relation only up to 2400 AU (Poveda et al. 1997).[1]

The different values of the major semiaxes of the solar neighborhood binaries at which both groups begin to depart from Oepik's distribution were interpreted as due to dissolution effects which, with the passage of time, tend to eliminate the widest systems. Weinberg et al. (1987) have modeled the evo-

[1] To estimate the ages of these groups of nearby stars, we computed their velocity dispersions. For the younger pairs we found $\sigma = 23.5$ km s^{-1}, a value similar to that of the F4 V and F5 V stars in Gliese's catalogue. The nuclear lifetimes for this group of stars are about 5 Gy (Maeder & Meynet 1988). Under the hypothesis of a constant rate of star formation the mean age of the younger group is then about 2.5 Gy. Similarly, the velocity dispersion of the older pairs was found to be $\sigma = 53$ km s^{-1}, comparable to that of the G V stars, from which a mean age of 7 Gy was calculated for this group.

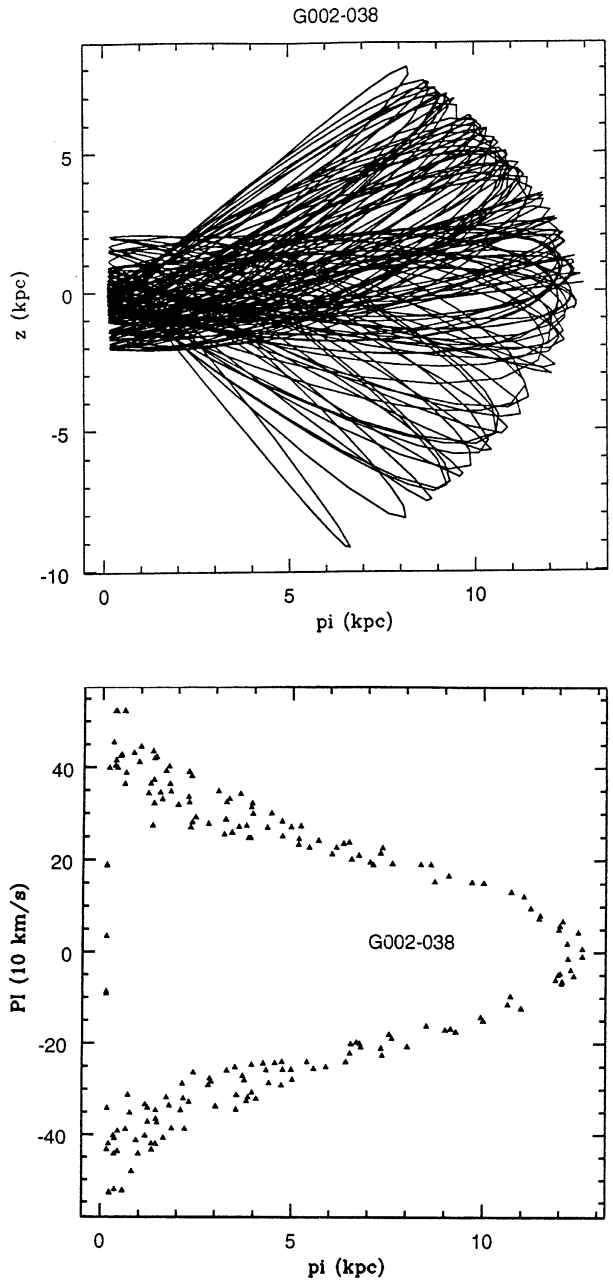

Fig. 11. Meridional orbit and surface of section of G2-38. This system shows chaotic behaviour.

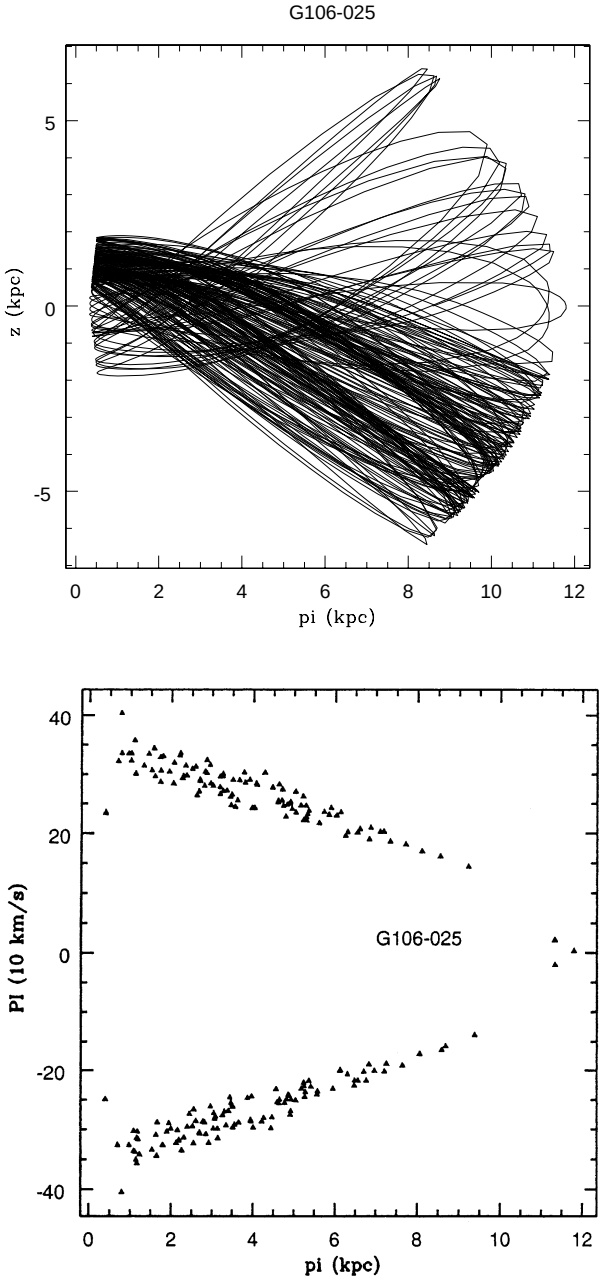

Fig. 12. Meridional orbit and surface of section of G106-25. This system also shows chaotic behaviour.

lution of binaries subject to perturbations by molecular clouds. From Fig. 6 in their paper one can see that systems with original separations of 2000 AU are practically unperturbed after 10 Gy, while systems with original separations of 12 900 AU have a probability of survival of about 0.1 after the same period of time. These results of the calculations of Weinberg et al. are consistent with the distributions of separations of the youngest and oldest systems in the solar neighborhood.

The much larger value of $\langle a \rangle$ at which the distribution begins to depart from Oepik's relation, as observed for the high-velocity, metal-poor wide binaries here studied, can be due to several effects. One is the relatively small time spent by the binaries within the galactic disk, which is where most of the dynamical perturbations take place. Another is the large relative velocity with which the encounters with perturbers occur, resulting in smaller energy exchanges per encounter.

In order to test the importance of each of these effects, we have used the galactic orbits to compute the fraction of their total lifetimes (t_D/t_T) that the binaries spend within the galactic disk, i.e., the region where the density of perturbers is highest. We divided the present sample into three equally populated groups ($n \approx 44$), according to the fraction of their lifetimes they spend within $|z| < 500$ pc. The first group, Group I, with $t_D/t_T \simeq 1.0$ contains the most disk-like stars; Group II, with

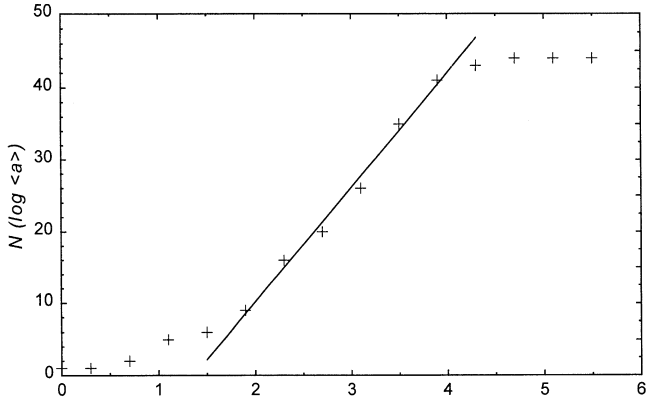

Fig. 13. Cumulative distribution of the expected values of the logarithms of the major semiaxes for Group I, the most disk-like binaries.

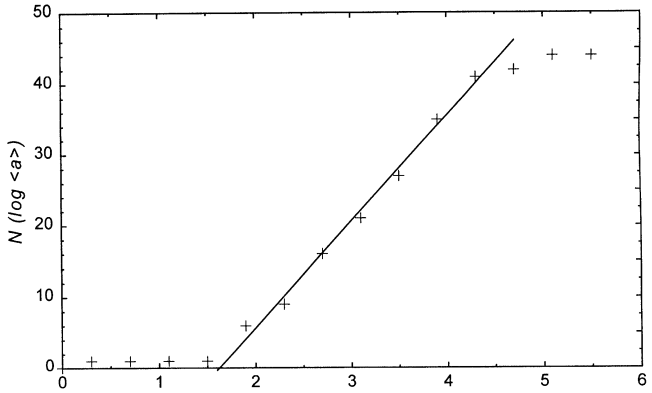

Fig. 14. Cumulative distribution of the expected values of the logarithms of the major semiaxes for Group II, the most halo-like binaries.

$\overline{t_D/t_T} \simeq 0.26$, the most halo-like stars; and the third group those of intermediate character. To maximize the contrast, the intermediate group was disregarded. Note that this grouping does not take into account any information on the metallicities of the stars, but depends just on the geometry of their galactic orbits. For Group I, the cumulative distribution of major semiaxes follows Oepik's relation only to $\langle a \rangle_{\max} < 8\,000$ AU, whereas for Group II Oepik's relation holds up to $\langle a \rangle_{\max} < 20\,000$ AU.

Table 1. The maximum major semiaxes $\langle a \rangle_{\max}$ for which Oepik's distribution holds, as found in three groups of old binaries

Groups	$\overline{t_D/t_T}$	σ (km s^{-1})	$\langle a \rangle_{\max}$ (AU)
Oldest local			
Binaries	1	53	2 400
I	1	77	8 000
II	0.26	204	20 000

These results, displayed in Figs. 13 and 14, strongly indicate that the absence of perturbers at high values of $|z|$ preserves the primeval distribution of major semiaxes, i.e., Oepik's relation.

The importance of the relative velocities of the encounters with massive perturbers in preserving Oepik's distribution has been tested as follows. We first note that the velocity dispersions of the wide *older* pairs of the solar neighborhood (with mean ages of about 7 Gy) was found to be $\sigma = 53$ km s^{-1}; we assume this velocity to be the typical velocity of encounters of these stars with massive molecular clouds in the disk, which move essentially with the local circular velocity. For comparison, the velocity dispersions of the binaries in Group I is $\sigma = 77$ km s^{-1}, while that of Group II is $\sigma = 204$ km s^{-1}. These results are summarized in Table 1, where we list median values of t_D/t_T for each group.

Table 1 clearly shows the importance of the small space density of perturbers, and of the large relative velocity of encounters, in preserving the primeval distribution of major semiaxes.

It is interesting to note that the distribution of absolute magnitudes of the secondaries extends all the way to about $M_V = 15$ (see Fig. 2). The sample of faint secondaries in Table 2 well deserves to be observed photometrically and spectroscopically to better determine the faint end of the main sequence.

Acknowledgements. We thank the referee, Dr. S.C. Ryan, for his thoughtful comments, which led to several improvements of this paper. Our sincere thanks go to G. Cordero, A. Nigoche, L. Rivera and A. Hernández for valuable assistance. We acknowledge partial financial support for this research from Conacyt through Grant Nr. 25502-E.

Appendix.

Table 2. A Catalogue of Wide Binaries Among High-Velocity Metal-Poor Stars

HIP	Id	N	d (pc)	M_{V_p}	M_{V_s}	s ($''$)	$\langle a \rangle$ (AU)	[Fe/H]	Age (10^9 yr)	v_p (km s^{-1})	R_{max} (kpc)	$\lvert z_{max} \rvert$ (pc)	e	Pop	Notes
(1)	(2)	(3)	(4)	(5)	(6)	(7)	(8)	(9)	(10)	(11)	(12)	(13)	(14)	(15)	(16)
754	471	2	45.3	4.5	8.8	30.	1902	−0.15	11.6	33.4	8.6	258	0.11	d	2
911	G266-60	2	251.	4.8	6.2	8.5	2986	−1.54		361.3	31.6	3122	0.92	h	1
2663	3074	2	36.2	3.6	6.0	6.	304	0.15	4.4	90.9	9.3	146	0.34	d	2
2941	3443	2	15.5	4.6	4.6	0.67	10.4	−0.13	14.4	91.0	9.9	209	0.31	d	2,O
3550	G32-46	2	63.	5.8	13.4	62.	5467	−0.16		69.8	9.7	350	0.22	d	1
5140	6517	2	82.	4.4	7.8	23.	2640	−0.33	15.9	53.5	8.6	528	0.16	td	1
6130	7895	2	27.7	5.8	9.3	28.	1084	−0.08		49.7	8.6	112	0.21	d	2
	G2-38	2	153.	5.4	10.5	24.	5139	−1.28		303.0	12.9	8058	0.98	h	1,5
7869	10607	2	71.4	4.1	9.1	22.	2198	−0.83		183.7	8.6	4562	0.51	h	2
9094	11964	2	34.0	3.8	8.4	29.	1379	0.15	13.1	80.5	12.4	201	0.26	d	2
9971	G72-58	2	57.	6.2	7.0	22.	1755	−0.45		86.5	8.6	679	0.32	td	1
	G4-16	2	134.	7.0	12.3	41.	7689	−1.76		147.8	8.6	468	0.67	h	1
11137	14786	2	57.3	5.0	5.4	34.	2727	−0.3		65.4	12.6	657	0.22	td	2
12114	16160	3	7.2	6.5	12.4	170.	1715	−0.09		78.5	11.6	736	0.22	td	2
12114	16160	3	7.2	6.5	>11.5	0.26	1.9								3,O
12411	16714	2	40.0	5.3	13.4	31.	1738	−0.17		81.1	8.9	311	0.32	td	2
13081	17382	2	22.4	5.8	12.9	20.	626	−0.09		17.7	8.6	68	0.07	d	2
14342	19059	2	99.7	3.6	7.6	1.	140	−0.44		104.5	8.7	2366	0.10	h	2
15126	G77-35	2	79.1	5.7	11.3	78.	8686	−0.81		155.1	12.7	785	0.48	td	2
15253	20369	2	78.	4.8	7.3	2.	218	−0.55	19.2	117.8	9.9	76	0.43	td	1
15394	20512	2	57.0	3.6	10.7	135.	10772	−0.11	19.1	72.4	8.8	673	0.23	td	2
15396	W1828	2	214.	4.6	8.3	185.	55410	−2.05		417.5	9.6	5202	0.12	h	1
15371	20807	2	12.1	4.8	5.2	310.	5241	−0.26		74.0	9.5	321	0.24	d	2
15572	20727	2	50.7	4.9	11.5	81.	5752	−0.29	11.7	60.5	8.7	444	0.21	td	2
15683	G6-3	2	73.	6.6	14.5	26.	2656	0.21		92.7	9.3	593	0.32	td	1
	20835	2	79.	4.3	10.5	10.	1106	−0.01	11.3	87.2	12.7	817	0.26	td	1
16467	21727	2	53.8	5.0	9.1	16.	1205	0.01	10.5	70.2	8.9	318	0.27	d	2
	G6-22	2	108.	5.9	10.7	3.	453	−0.35		143.6	10.5	891	0.48	td	1
17666	23439	2	24.5	5.7	6.8	8.	274	−1.23		151.4	9.6	1603	0.51	h	2
18824	25535	3	52.2	3.1	3.7	1.9	139	−0.11	9.8	86.9	8.7	1094	0.25	td	2
18824	25535	3	52.2	3.1	14.9	64.	4678								
19255	G39-1	3	20.6	5.6	7.4	3.6	74.1	−0.13		24.2	9.0	27	0.08	d	2,O
19255	G39-1	3	20.6	5.6	3.8	720	20739								
19849	26965	3	5.0	5.9	10.8	82.	578	−0.04		111.2	12.7	624	0.34	td	2
19849	26965	3	5.0	10.8	12.6	6.9	34.8								O
	283702	2	80.	6.1	8.3	16.	1791	−0.23		92.1	8.6	144	0.41	td	1
	G85-17	2	103.	5.4	12.8	133.	19173	−0.48		101.9	8.7	2000	0.20	h	1
	31208	2	34.	5.5	5.8	16.	761	−0.05		53.0	8.7	41	0.22	d	1
24819	34673	2	16.9	6.6	9.6	4.	94	0.48		90.6	9.7	363	0.31	d	2
25137	G96-35	2	62.0	5.3	8.8	76.	6591	−0.56		80.6	12.4	1196	0.22	h	2
26018	36524	2	46.1	5.5	7.3	4.	258	−0.17		56.5	8.7	607	0.16	td	2
26501	37706	2	25.3	5.3	7.9	5.5	194	−0.29		63.1	10.4	253	0.19	d	2
26907	38014	2	31.3	6.1	11.2	53.	2325	−0.16		88.9	8.5	130	0.40	td	2
28671	250792	2	39.	6.4	9.8	7.	382	−1.18		258.6	16.4	1822	0.76	h	1
28940	G106-25	2	70.	6.6	10.4	12.	1176	0.28		265.5	11.8	6401	0.94	h	1,5
31740	G101-47	2	83.9	5.5	13.7	62.	7280	−0.32	18.1	131.8	9.9	784	0.46	td	2
32423	263175	2	25.0	6.8	10.3	31.	1084	−0.19		70.7	13.7	916	0.24	td	2
32650	49409	3	50.1	4.4	5.2	0.77	38.6	−0.31		128.3	12.6	1116	0.37	td	2,O
32650	49409	3	50.1	4.4	12.4	27.	1893								
34065	53705	3	16.2	4.5	8.1	193.	4389	−0.06		75.7	8.8	156	0.30	d	2
34065	53705	3	16.2	4.5	5.6	21.	478								
35599	56196	2	84.6	4.3	11.5	58.	6868	0.01	6.7	117.9	10.0	175	0.42	td	2
35756	G89-14	2	180.	4.1	10.4	34.	8565	−1.61		262.7	11.7	8661	0.96	h	1

Table 2. Continued.

HIP	Id	N	d (pc)	M_{V_p}	M_{V_s}	s ($''$)	$\langle a \rangle$ (AU)	[Fe/H]	Age (10^9 yr)	v_p (km s^{-1})	R_{max} (kpc)	$\lvert z_{max} \rvert$ (pc)	e	Pop	Notes
(1)	(2)	(3)	(4)	(5)	(6)	(7)	(8)	(9)	(10)	(11)	(12)	(13)	(14)	(15)	(16)
36165	59099	2	39.7	4.0	4.6	17.	944			76.5	9.4	686	0.22	td	2
36357	G90-1	3	17.6	6.5	2.2	757.	18594	−0.28		39.6	10.9	259	0.14	d	2
36357	G90-1	3	17.6	2.2	10.6	2.8	68.8								
37671	G112-43	2	167.	4.1	5.1	12.	2805	−1.41	17.6	290.3	21.6	17469	0.52	h	1
	G40-14	2	235.	4.3	12.2	98.	32233	−2.34	20.3	413.2	16.4	1444	0.70	h	1
46853	82328	2	13.5	2.5	12.9	5.	94	−0.21	3.8	56.2	9.3	220	0.18	d	2
47225	83529	2	34.1	4.3	9.4	4.	191	−0.33		49.9	8.6	437	0.16	td	2
	G43-7	2	120.	6.3	13.0	15.	2519	−0.66		178.4	13.9	340	0.56	td	1
49668	87998	2	37.8	4.4	8.1	4.7	248	−0.23	10.7	55.5	8.7	620	0.15	td	2
53165	94220	2	55.2	4.4	6.1	1.	77.3	−0.02	8.7	73.3	9.7	403	0.23	td	2
	G45-48	2	92.	5.4	8.9	18.	2318	−0.16		103.7	14.5	602	0.33	td	1
57443	102365	2	9.2	5.1	15.7	23.	297	−0.22		58.4	9.4	139	0.20	d	2
58401	104006	2	31.9	6.4	13.4	23.	1027	−0.57		189.1	8.5	24	0.88	h	2
58962	105004	3	135.	4.7	8.5	12.	2267	−1.09		266.9	9.5	5962	0.93	h	1,5
58962	105004	3	135.	4.7	7.8	1.8	340								
59126	105304	2	41.5	6.5	15.3	66.	3836	−0.1		71.5	8.9	206	0.28	d	2
59233	G59-1	2	56.	5.8	10.3	16.	1254	−0.78		91.6	10.5	329	0.29	td	1
59532	106116	2	33.9	4.8	10.3	2.	95	0.14	8.	113.3	13.2	743	0.34	td	2
62041	G59-36	2	75.	6.4	14.8	12.	1260	−0.21		68.6	8.6	375	0.28	td	1
62882	111980	2	80.1	3.8	7.8	1.9	213	−0.95	19.4	356.1	22.0	9995	0.94	h	2
(63239)	112573	2	73.1	4.7	5.9	58.	5934	−0.3		84.5	11.6	320	0.26	d	2,4
63366	112758	2	21.0	5.9	11.1	1.4	41.2	−0.28		73.9	10.1	242	0.23	d	2
64345	114606	2	61.1	4.8	9.1	82.	7015	−0.55	20.9	164.4	14.6	1898	0.47	h	2
64386	G61-38	2	69.9	5.7	7.5	446.	43652	−0.74		117.5	11.0	511	0.37	td	2
64797	115404	2	11.2	6.3	10.1	4.	62.9	−0.16		48.8	11.1	50	0.17	d	2
67246	120066	2	30.6	3.9	7.5	486.	20828	−0.22		68.0	9.1	195	0.25	d	2
67408	120237	2	28.3	4.3	8.2	12.	475	−0.22	6.1	59.8	8.8	33	0.24	d	2
69220	123682	3	48.8	4.9	7.0	57.	3893	−0.14	10.7	79.8	9.0	795	0.24	td	2
69220	123682	3	48.8	4.9	11.0	4.	273								
71505	128580	2	99.	4.6	5.7	27.	3741	−0.08	9.6	140.5	11.3	158	0.46	d	1
71735	128674	2	27.4	5.2	9.0	490.	18825	−0.38		74.1	11.1	922	0.19	td	2
74199	G15-10	2	132.	6.4	6.6	677.	125073	−2.14		306.7	15.6	7088	0.87	h	1
74235	134439	2	29.3	6.7	7.4	302.	12380	−1.33		592.2	67.0	6410	0.86	h	2
74549	134928	2	51.	4.9	5.0	17.	1213	0.11	16.3	81.6	9.4	216	0.28	d	1
74537	135204	2	17.3	5.4	5.4	0.1	2.4	0.03	17.3	116.0	9.3	97	0.46	td	2
75069	136378	2	44.6	6.0	9.3	190.	11856	−0.38		58.9	9.5	656	0.14	td	2
77282	140690	2	48.2	4.7	4.9	0.2	13.5	0.00	9.4	69.6	8.9	77	0.28	d	2
	G16-25	2	256.	6.3	8.7	1.5	537	−1.89		515.9	19.9	6958	0.43	h	1
80630	148408	2	66.	5.5	11.0	23.	2125	−0.6		186.8	10.8	313	0.67	td	1
83591	154363	2	10.8	7.5	9.4	184.	2770			74.8	8.9	300	0.28	d	2
85378	158226A	2	68.9	4.3	5.7	67.	6463	−0.64	18.1	128.9	9.0	1489	0.43	h	2
87533	162756	2	66.3	3.5	7.0	1.	92.8	−0.18	10.6	133.3	9.2	526	0.51	td	2
88010	163810	2	78.	5.2	6.5	0.3	32.8	−1.4		368.9	18.8	11360	0.96	h	1,5
88937	165896	2	40.4	4.6	10.1	4.6	260	−0.59		56.5	8.5	210	0.23	d	2
89000	166285	3	46.9	2.3	8.3	7.2	473	−0.40		36.2	8.5	223	0.13	d	2
89000	166285	3	46.9	2.3	6.6	104.	6808								
91360	171999	2	37.1	5.5	11.9	36.	1868	0.05		76.1	8.5	57	0.35	d	2
91605	G206-38	2	23.9	6.6	9.9	9.	301	−0.36		108.2	13.2	484	0.33	td	2
92960	175617	2	74.7	5.8	10.6	33.	3452	−0.45		145.6	11.3	311	0.47	td	2
93827	177758	2	38.8	4.3	10.4	0.2	10.9	−0.66	15.5	77.9	8.8	43	0.32	td	2
96333	184392	3	72.	4.7	9.3	40.	4031	−0.43	19.5	102.5	8.8	157	0.43	td	1
96333	184392	3	72.	4.7	6.7	1.4	141								

Table 2. Continued.

HIP	Id	N	d (pc)	M_{V_p}	M_{V_s}	s ($''$)	$\langle a \rangle$ (AU)	[Fe/H]	Age (10^9 yr)	v_p (km s^{-1})	R_{max} (kpc)	$\lvert z_{max} \rvert$ (pc)	e	Pop	Notes
(1)	(2)	(3)	(4)	(5)	(6)	(7)	(8)	(9)	(10)	(11)	(12)	(13)	(14)	(15)	(16)
96402	184768	2	39.1	4.6	10.8	3.	164	−0.08	10.3	64.3	8.7	257	0.25	d	2
97940	188268	3	47.3	5.4	5.7	163.	10802	−0.02		57.2	9.1	290	0.19	d	2
97940	188268	3	47.3	5.4	8.1	76.8	5089								
98767	190360	2	15.9	4.7	14.3	178.	3959	0.16	7.8	64.4	8.5	990	0.11	td	2
99029	190333	2	75.	4.9	6.6	2.	210	−0.36	19.3	98.4	8.9	316	0.39	td	1
99461	191408	2	6.1	6.4	12.5	8.	67.7	−0.29		130.1	11.3	1139	0.38	h	2
100970	195019	2	37.4	4.0	7.5	3.	157	−0.11	8.2	96.0	9.2	425	0.35	d	2
104214	201091	3	3.5	7.5	8.5	24.6	85.6			95.0	10.1	13	0.32	d	2,O
104214	201091	3	3.5	7.5	¿19	0.014	0.049								6,O
104660	201889	2	55.7	4.3	6.3	1.3	101	−0.79	24.6	142.3	10.9	476	0.48	td	2
106074	G126-2	3	50.7	7.6	12.1	0.7	49.7			278.0	8.8	1919	0.80	h	2,5
106074	G126-2	3	50.7	7.6	9.1	1.1	80.2								
	G26-8	2	72.	6.2	9.0	9.5	957	−0.23		104.9	9.9	52	0.37	td	1
106335	G26-9	3	49.4	6.9	12.5	132.	9119	−1.19		133.1	10.9	97	0.45	h	2
106335	G26-9	3	49.4	6.9	8.6	0.7	48.4								
	G18-24	2	119.	6.6	11.0	99.	16489	−1.49		201.9	10.4	757	0.76	h	1
113231	216777	2	34.8	5.3	13.6	42.	2047	−0.4		81.0	9.8	154	0.28	td	2
113280	216863	2	32.2	6.3	7.7	5.	225	0.09		28.4	8.5	250	0.09	d	2
114980	219495	2	27.3	6.8	6.6	71.	2709			82.5	8.5	380	0.35	d	2
114962	219617	3	39.	6.2	13.8	15.	819	−1.42		237.9	12.9	575	0.78	h	1
114962	219617	3	39.	6.2	6.4	0.48	18.7								O
115012	219657	2	55.2	4.2	5.8	1.	77.3	0.02	8.7	72.4	8.9	155	0.29	d	2
115684	G128-64	2	88.6	4.9	7.2	260.	32230	−0.03	15.	103.4	10.7	334	0.32	d	2
116421	221830	2	32.3	4.3	11.4	8.	362	−0.53	17.4	131.2	9.0	1407	0.46	h	2
146	224927	2	99.	4.0	4.4	0.17	16.8	−1.18		174.0	11.2	318	0.60	h	1,O
171	224930	2	12.4	5.3	10.6	0.83	10.3	−0.89		65.7	8.5	305	0.28	d	2,O

O Orbit available, the actual value of a is listed.
1 Distance from Schuster et al.
2 Distance from Hipparcos.
3 Visual magnitude of secondary estimated by Lippincott (1969). Golimowski et al. (1995) obtain $M_k = 9.5$.
4 Hipparcos number corresponds to secondary.
5 Galactic orbit is chaotic.
6 Orbits computed by Strand (1957). Lower bound to magnitude of secondary estimated from its mass.

References

Abt H.A., Levy S.G., 1976, ApJS 30, 273
Abt H.A., Willmarth D., 1987, ApJ 318, 786
Allen C., Santillán A., 1993, Rev. Mex. Astron. Astrofís. 22, 255
Allen C., Poveda A., Herrera M.A., 1997, In: Docobo J.A., Elipe A., McAlister H. (eds) (eds.) Visual Double Stars: Formation, Dynamics and Evolutionary Tracks. Kluwer, Dordrecht, p. 133
Allen C., Schuster W.J., 2000, in preparation
Carney B., 1983, AJ 101, 623
Couteau P., 1960, J. des Observateurs 43, No. 3
Dommanget J., Nys O., 1994, Components of Double and Multiple stars Catalogue (CCDM)
European Space Agency (ESA), 1997, The Hipparcos and Tycho Catalogues, SP-1200
Gliese W., Jahreiss H., 1991, In: Brotzman L.E., Gessner S.E. (eds.) Selected Astronomical Catalogues Vol. I, NSSC, NASA, GSFC (GJ91)
Golimowski D.A., Nakajima T., Kulkarni S.R., Oppenheimer B.R., 1995, ApJ 444, L101
Hillenbrand L., 1997, AJ 113, 1733
Laird J.B., Carney B.W., Latham D.W., 1988, AJ 95, 1843
Larson R.V., 1995, MNRAS 272, 213
Lavalley C., 1994, Bachelor's Thesis, UNAM, p. 93
Lippincott S.L., 1969, BAAS 1, 199
Luyten W.J., 1987, LDS Catalogue
Luyten W.J., 1979, NLTT Catalogue Parts I, II
Luyten W.J., 1980, NLTT Catalogue Parts III, IV
Maeder A., Meynet, G., 1988, A&AS 76, 411
Martin E., Rebolo R., 1992, ASP Conference Series 32, 336
Nigoche A., 2000, Master's Thesis, UNAM
Nissen P.E., Twarog B.A., Crawford D.L., 1987, AJ 93, 634
Nissen P.E., Schuster W.J., 1991, A&A 251, 457
Oepik E.J., 1924, Tartu Obs. Publ, 25
Oort J.H., 1926, Pub. Kapteyn Astr. Lab., Groningen, 40
Perryman M.A., Brown A.G., Lebreton Y., et al., 1998, A& 331, 81
Poveda A., Allen C., Herrera, M.A., 1997, In: Docobo J.A., Elipe A., McAlister H. (eds.) Visual Double Stars: Formation, Dynamics and Evolutionary Tracks. Kluwer, Dordrecht, p. 191
Ryan S.C., 1992, AJ 104, 1144

Ryan S.C., 1989, AJ 98, 1693
Sandage A., Fouts G., 1987, AJ 93, 74
Schuster W.J., Allen C., 1997, A&A 319, 796
Schuster W.J., Nissen P.E., 1988, A&AS 73, 225
Schuster W.J., Nissen P.E., 1989a, A&A 221, 65
Schuster W.J., Nissen P.E., 1989b, A&A 222, 69
Schuster W.J., Parrao L., Contreras M.E., 1993, A&AS 97, 951
Strand K. Aa., 1957, AJ 62, 35
Stryker L., Hesser J., Hill G., Garlick G., O'Keefe L., 1985, PASP 97, 247
Valtonen M., 1997, In: Docobo J.A., Elipe A., McAlister H. (eds.) Visual Double Stars: Formation, Dynamics and Evolutionary Tracks. Kluwer, Dordrecht, p. 241
VandenBerg D.A., 1985, ApJS 58, 711
Weinberg M.D., Shapiro S.L., Wasserman I., 1987, ApJ 312, 367